



Research paper

CpG sites with continuously increasing or decreasing methylation from early to late human fetal brain development



Eberhard Schneider^a, Marcus Dittrich^{a,b}, Julia Böck^a, Indrajit Nanda^a, Tobias Müller^b, Larissa Seidmann^c, Tim Tralau^{c,d}, Danuta Galetzka^e, Nady El Hajj^a, Thomas Haaf^{a,*}

^a Institute of Human Genetics, Julius Maximilians University, 97074 Würzburg, Germany

^b Department of Bioinformatics, Julius Maximilians University, 97074 Würzburg, Germany

^c Department of Pathology, University Medical Center, 55131 Mainz, Germany

^d Rehabilitation Clinic for Children and Adolescents, 25980 Westerland/Sylt, Germany

^e Department of Radiation Oncology and Radiotherapy, University Medical Center, 55131 Mainz, Germany

ARTICLE INFO

Article history:

Received 22 April 2016

Received in revised form 28 June 2016

Accepted 23 July 2016

Available online 25 July 2016

Keywords:

Autism

Fetal brain development

Frontal cortex

DNA methylation dynamics

Methylome

ABSTRACT

Normal human brain development is dependent on highly dynamic epigenetic processes for spatial and temporal gene regulation. Recent work identified wide-spread changes in DNA methylation during fetal brain development. We profiled CpG methylation in frontal cortex of 27 fetuses from gestational weeks 12–42, using Illumina 450K methylation arrays. Sites showing genome-wide significant correlation with gestational age were compared to a publicly available data set from gestational weeks 3–26. Altogether, we identified 2016 matching developmentally regulated differentially methylated positions (m-dDMPs): 1767 m-dDMPs were hypermethylated and 1149 hypomethylated during fetal development. M-dDMPs are underrepresented in CpG islands and gene promoters, and enriched in gene bodies. They appear to cluster in certain chromosome regions. M-dDMPs are significantly enriched in autism-associated genes and CpGs. Our results promote the idea that reduced methylation dynamics during fetal brain development may predispose to autism. In addition, m-dDMPs are enriched in genes with human-specific brain expression patterns and/or histone modifications. Collectively, we defined a subset of dDMPs exhibiting constant methylation changes from early to late pregnancy. The same epigenetic mechanisms involving methylation changes in cis-regulatory regions may have been adopted for human brain evolution and ontogeny.

© 2016 The Authors. Published by Elsevier B.V. This is an open access article under the CC BY-NC-ND license (<http://creativecommons.org/licenses/by-nc-nd/4.0/>).

1. Introduction

The complexity of the human brain and cognitive functions is interrelated with temporally and spatially highly coordinated gene regulation during fetal brain development. Recent studies have elucidated the underlying epigenetic mechanisms, in particular the neurodevelopmental trajectories in fetal brain DNA methylation (Numata et al., 2012; Pidsley et al., 2014; Spiers et al., 2015; Jaffe et al., 2016) and gene transcription (Colantuoni et al., 2011; Lambert et al., 2011; Miller et al., 2014; Jaffe et al., 2015). Accumulating evidence suggests that DNA methylation in human prefrontal cortex is highly dynamic during the first and second trimester, compared to the adult brain where most developmentally dynamic genes display relatively small changes with age. These

developmentally regulated differentially methylated positions in the genome have been referred to as dDMPs (Spiers et al., 2015). CpG islands (CGIs) are 500–2000 bp DNA segments with high CpG density that are associated with most mammalian genes. Methylation of these cis-regulatory regions during development or disease processes is associated with posttranslational histone modifications that lead to a locally condensed inactive chromatin structure and gene silencing (Jaenisch and Bird, 2003; Weber et al., 2007). In contrast, gene body methylation is positively correlated with transcription and may have functions in silencing transposable elements and regulating splicing (Yoder et al., 1997; Laurent et al., 2010; Jones, 2012). The epigenome is the sum of the epigenetic modifications in a cell type or tissue which bring the phenotype into being. One important hallmark of the epigenome is its enormous plasticity in response to internal (i.e. during development) and environmental factors (Haaf, 2006; Feil and Fraga, 2012).

It is plausible to assume that genes associated with dDMPs play an important role for brain development and that misregulation in sensitive time windows may interfere with normal brain function. Indeed, dDMPs were found to be enriched in genomic regions that have been associated with schizophrenia and autism (Spiers et al.,

Abbreviations: ASD, autism spectrum disorder; BA, Brodmann area; CGI, CpG island; CpG, cytosine phosphate guanine; dDMP, developmentally regulated differentially methylated position; DMR, differentially methylated region; m-dDMP, matching dDMP.

* Corresponding author at: Institute of Human Genetics, Julius-Maximilians-Universität Würzburg, Biozentrum, Am Hubland, 97074 Würzburg, Germany.

E-mail address: thomas.haaf@uni-wuerzburg.de (T. Haaf).

2015; Hannon et al., 2016). Both schizophrenia and autism have a high heritability (up to 80%) and are thought to have a basis in neurodevelopmental disturbances of the fetal brain (Fatemi and Folsom, 2009; Werling and Geschwind, 2013). Schizophrenia is characterized by abnormalities in the perception or expression of reality, affecting cognitive and psychomotor functions (<http://www.icd10data.com>). Autism spectrum disorder (ASD) is characterized by deficits in social interactions, communicative impairments and stereotypic behavioral patterns (Zafeiriou et al., 2013). It is hypothesized that the disease manifests when the sum of adverse genetic, epigenetic and/or environmental factors exceeds a critical threshold (Loke et al., 2015). In contrast to schizophrenia and autism, Alzheimer's disease is a neurodegenerative disorder resulting from progressive dysfunction, degeneration and death of neurons in the human brain. Epigenetic modifications are altered during ageing and Alzheimer pathogenesis (Lunnon and Mill, 2013; Levine et al., 2015).

Here we performed a methylation array analysis of fetal cortex samples to identify dDMPs and developmentally regulated genes. There are already several studies (Numata et al., 2012; Pidsley et al., 2014; Spiers et al., 2015; Jaffe et al., 2016) on the fetal brain methylome, however due to different techniques and tissue samples (brain region, gestational week, spontaneous vs. elective abortion), existing data sets are likely still polluted with false positives and false negatives. By comparing our results with the most comprehensive study using Illumina 450 K methylation arrays (Spiers et al., 2015), we defined a subset of approximately 3000 dDMPs showing significant changes in the same direction across fetal brain development.

2. Materials and methods

2.1. Subjects and sample preparation

This study was approved by the ethics committees of the Landesärztekammer Rheinland-Pfalz (no. 837.103.04_4261) and the Medical Faculty of the University of Würzburg, Germany (no. 262/14). Brain samples (Table 1) were obtained from excess material of fetal

autopsies. After determination of postmortem time (based on anamnestic data and autolytic processes) and gestational age (foot length measurements), cortex tissue was dissected from the frontal lobe (BA10). Chromosome disorders were excluded by karyotype analyses of primary fibroblast cultures from Achilles tendon.

Tissue samples were disrupted using the Precellys tissue DNA kit (PEQLAB, Erlangen, Germany). Genomic DNA was isolated with the DNeasy blood and tissue kit (Qiagen, Hilden, Germany). Bisulfite conversion was performed using one microgram DNA and the EZ-96 DNA methylation kit (Zymo Research, Irvine, CA, USA). Total RNA was isolated with the RNeasy lipid and tissue mini kit (Qiagen). Amount and quality of DNA and RNA were analyzed with an Agilent 2100 Bioanalyzer (Agilent, Santa Clara, CA, USA) system.

2.2. Microarray analysis

After bisulfite conversion, the 27 samples were whole-genome amplified, enzymatically fragmented, and hybridized to two Illumina HumanMethylation450 (450K) BeadChips according to the manufacturer's protocol (Illumina, San Diego, CA, USA). The arrays were scanned with an Illumina iScan. Microarray data (NCBI GEO accession no. GSE73747) were exported as idat files and preprocessed using the RnBeads pipeline with default settings (Assenov et al., 2014). 4713 sites overlapping SNPs, 3156 sites not in the CpG context and 523 probes flagged as unreliable based on the corresponding detection *P* value were removed. Furthermore, 11,169 probes on the sex chromosomes were excluded, leaving a total number of 465,572 probes (covering 99% of RefSeq genes with promoter, first exon, gene body, 5' and 3' UTRs and 96% of CpG islands) for subsequent analyses. The signal intensity values were normalized using the SWAN normalization method (Maksimovic et al., 2012), as implemented in the minfi package (Aryee et al., 2014). Differential methylation analysis has been performed using the moderated *t*-test model as implemented in the limma package (Ritchie et al., 2015) based on β values of the fetal samples. CpG sites exhibiting a linear correlation >0.7 (FDR adjusted $P < 0.05$) with gestational age (weeks) were considered as dDMPs.

Table 1
Fetal frontal cortex samples.

Cortex sample	Sex	Gestational week	Cause of death	Abortion	Postmortem time (h)
1	F	12	Amniotic infection	Induced	36
2	F	13	Amniotic infection	Spontaneous	24–48
3	M	15	Retroplacental hemorrhage	Spontaneous	48–72
4	F	15	Premature placental abruption	Spontaneous	24–48
5	M	15	Chorioamnionitis with necrosis	Spontaneous	24–48
6	F	17	Premature rupture of membranes	Induced	<24
7	F	17	Premature placental abruption	Induced	<24
8	M	18	Amniotic infection	Spontaneous	<24
9	F	18	Premature rupture of membranes and amniotic infection	Spontaneous	24–48
10	M	18	Premature rupture of membranes	Induced	<24
11	M	18	Amniotic infection	Spontaneous	<24
12	M	19	Premature rupture of membranes and chorioamnionitis	Spontaneous	24–48
13	F	20	Not known	Induced	<24
14	F	20	Premature placental abruption	Spontaneous	<24
15	M	20	Amniotic infection	Spontaneous	<24
16	M	20	Not known	Induced	24–48
17	F	20	Amniotic infection	Induced	<24
18	M	21	Not known	Induced	<24
19	M	21	Not known	Spontaneous	72
20	F	22	Premature rupture of membranes	Spontaneous	24–48
21	F	23	Premature rupture of membranes and chorioamnionitis	Spontaneous	24–48
22	F	23	Preterm labor	Spontaneous	48
23	F	23	Preterm labor	Spontaneous	48
24	M	24	Chorioamnionitis	Spontaneous	72
25	M	25	Premature placental abruption	Spontaneous	24–48
26	F	32	Umbilical cord stricture	Spontaneous	48
27	F	42	Placental insufficiency	Spontaneous	<24

2.3. Targeted RNA sequencing

A customized TruSeq RNA expression panel (Illumina Design Studio) with 25 assays (El Hajj et al., 2016) targeted *DNMT3B*, *NRSF/REST* and four internal control genes (as well as several other genes without m-dDMPs). All RNA samples were analyzed in technical duplicates. cDNAs were synthesized from 20 fetal frontal cortices using ProtoScript II Reverse Transcriptase (NEB, Frankfurt/Main, Germany). Subsequent steps were performed according to the TruSeq targeted RNA expression guide. The resulting TruSeq RNA library was sequenced for 50 cycles and dual-index 6 and 8 cycles using a Illumina MiSeq and the MiSeq Reagent Kit v3. Mapping and counting were performed with Illumina GenomeStudio software. Differential expression analysis was performed using the limma modeling framework (Ritchie et al., 2015) in combination with the “voom” method (Law et al., 2014) which has been specifically designed for the analysis of count data in RNAseq experiments.

2.4. Bioinformatic analysis

We compared the lists of significant dDMPs in our and a conceptually related study (Spiers et al., 2015). Only matching m-dDMPs which showed significant correlation with gestational age and the same direction of change (up- or downmethylation) in both data sets were considered for further analysis. To study their chromosomal distribution, the number of hypo- and hypermethylated dDMPs, respectively, on each chromosome was determined and compared to the number of 450K array probes on the respective chromosome. Subsequently, all CpG sites assessed by the array were aggregated into positional clusters with 5 or more sites. These positional clusters were then used for local enrichment analysis of m-dDMPs. Enrichment or depletion were calculated using Fisher's exact test with Bonferroni correction for multiple testing ($P < 0.05$). Genes associated with m-dDMPs were compared to candidate gene lists for autism (Autism database AutDB, 2015; <http://autism.mindspec.org/autdb>; Basu et al., 2009), schizophrenia (Schizophrenia Working Group of the Psychiatric Genomics Consortium, 2014), and Alzheimer's disease (AlzGene database, 2015; <http://www.alzgene.org>; Bertram et al., 2007).

A literature search identified genes with possible human-specific regulation in the adult primate brain (Supplemental Table S1). Altogether, we selected 2357 protein-coding genes (Nowick et al., 2009; Liu et al., 2012; Florio et al., 2015) and 153 microRNAs (Hu et al., 2011) with human-specific brain expression patterns, and 441 genes with human-specific histone methylation signatures at transcription start sites (Shulha et al., 2012).

3. Results

3.1. Methylation array analysis

Frontal cortex samples of 12 male and 15 female fetuses ranging from gestational weeks 12 to 42 (Table 1) were hybridized on Infinium HumanMethylation450 BeadChips. Altogether, 36,261 (7.8%) of 465,572 assessed CpG sites (excluding sex chromosomes) showed significant (adjusted $P < 0.05$, $R > 0.7$) methylation changes with gestational age. Localization of these dDMPs in the genome was classified into different categories: CpG islands, flanking CGI shores and shelves, and open sea (Fig. 1). Shores are regions up to 2 kb and shelves 2–4 kb from CGIs. The open sea represents CpGs not associated with an CGI. dDMPs were significantly (Fisher's exact test, $P < 0.01$) depleted in CpG islands (Fig. 1, upper panel). The majority, namely 24,467 (67.5%) dDMPs gained methylation and 11,794 (32.5%) lost methylation during intrauterine development. Although hypermethylated dDMPs were more frequent in all genomic regions (Fig. 1, lower panel), the most dramatic abundance was observed in CpG islands, where 95% of dDMPs were hypermethylated.

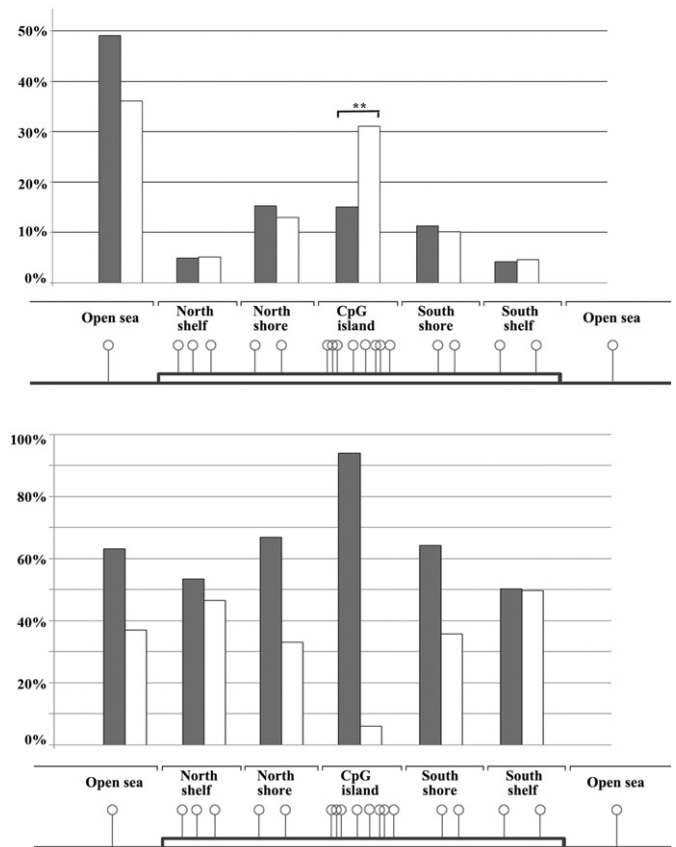


Fig. 1. The upper panel shows the distribution of dDMPs in the linear genome (x-axis). CpG islands are flanked by shores (up to 2 kb) and shelves (2–4 kb from CGI). The open sea represent the rest of the genome. Gray bars represent the percentage of dDMPs and white bars the percentage of assessed CpG sites in a specific region. CpG islands are significantly ($P < 0.01$) depleted of dDMPs. The lower panel shows the ratio of hypermethylated dDMPs (gray bars) versus hypomethylated dDMPs (white bars) in different genomic regions.

Approximately 36,000 dDMPs were identified in our data set, compared to 29,000 in an earlier methylation array study on fetal brain samples (Spiers et al., 2015). It is noteworthy that in our study the majority (67.5%) of dDMPs were hypermethylated, whereas in the published data set hypomethylated dDMPs (56.4%) predominated (Table 2). Of 6344 dDMPs which were significant in both data sets, more than half showed methylation changes in opposite direction. This leaves us with 1767 hypermethylated and 1149 hypomethylated dDMPs, matching between both studies (Fig. 2, upper panel). These 2916 matching m-dDMPs are continuously gaining or losing methylation from early to late gestational stages. When focusing on genes, 684 were associated with hypermethylated, 733 with hypomethylated, and 62 with both hyper- and hypomethylated m-dDMPs (in different regions of the gene). 216 m-dDMPs were mapped to 105 promoter regions (1.5 kb upstream to 0.5 kb downstream of transcriptions start sites), representing 74 hyper- and 31 hypomethylated m-dDMP promoters.

Table 2
Comparison of this study with a published data set.

	Spiers et al., 2015	This study	Matching dDMPs
Analyzed tissue	Brain	Frontal cortex	
Number of samples	179	27	
Sex	100 ♂, 79 ♀	12 ♂, 15 ♀	
Gestational weeks	3–26	12–42	
Number of analyzed probes	408,608	464,616	
Number of dDMPs	28,718	36,261	6344
Hypomethylated dDMPs	16,190	11,794	1149
Hypermethylated dDMPs	12,528	24,467	1767

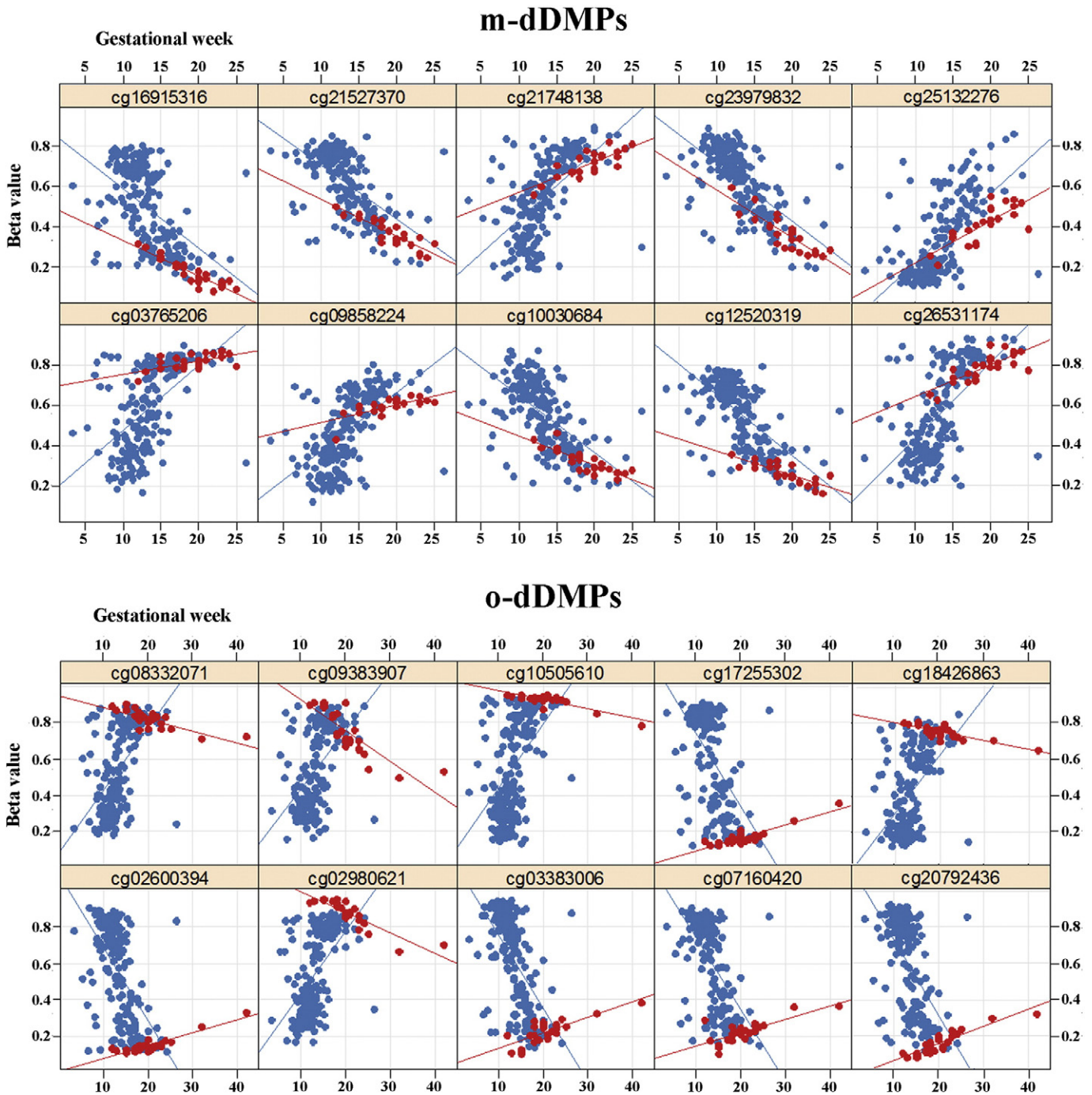


Fig. 2. Methylation trajectories of m-dDMPs and o-dDMPs. Blue dots represent fetal brain samples from a published data set (Spiers et al., 2015), red dots fetal cortex samples from our study. The x axis represents the gestational age in weeks and the y axis the methylation beta value. Regression lines are calculated for blue (median gestational age 13 weeks) and red samples (20 weeks), respectively. The upper panel demonstrates representative examples of m-dDMPs which exhibit significant methylation changes in the same direction in both studies. The bottom panel shows representative examples of o-dDMPs which exhibit significant methylation changes in opposite directions.

The majority of genic dDMPs were located in gene bodies, which are significantly enriched with dDMPs (Fig. 3, upper panel). The region upstream of the transcription start site (TSS1500 and TSS200) and the first exon were significantly depleted of dDMPs. With exception of UTRs, in particular the 3' UTR (with >60% hypomethylated dDMPs), the hypermethylated dDMPs predominated (Fig. 3, lower panel).

Another recent 450K array study (Mendioroz et al., 2015) focussing on methylation changes in Down syndrome (DS) showed dynamic methylation changes in fetal cerebrum (of 8 DS and 6 control samples). Following adjustment for DS status, 5775 developmentally regulated CpG sites were identified, including 657 of our 2916 m-dDMPs. This

overlap is highly significant ($P < 0.0001$) and moreover the direction of change for all overlapping (262 hyper- and 395 hypomethylated) m-dDMPs was identical in both studies. This indicates that the identified m-dDMPs are robust, reflecting developmental trajectories of the whole brain.

To determine whether the observed developmental methylation changes affect gene expression, targeted RNA sequencing was performed for two key regulatory genes with hypermethylated m-dDMPs promoters, namely the de novo methyltransferase *DNMT3B* and the neuron-restrictive silencer factor/RE1-silencing transcription factor *NRSF/REST*. Consistent with their increasing methylation, both genes

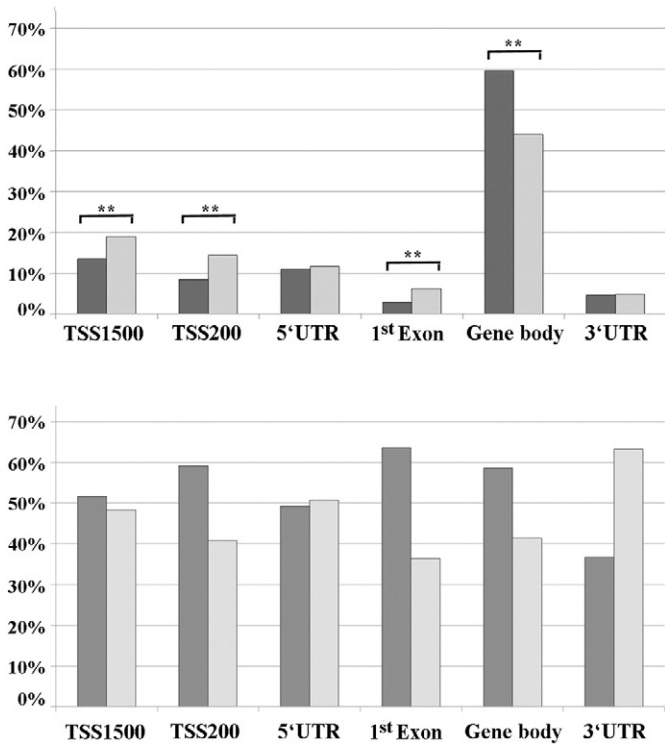


Fig. 3. The upper panel shows the distribution of dDMPs in different gene regions. TSS200 is the region from transcription start site (TSS) to -200 bp, TSS1500 from -200 bp to -1500 bp upstream of TSS. Gray bars represent the percentage of dDMPs and light bars the percentage of assessed CpG sites in a specific region. Gene promoters (TSS1500, TSS200 and 1st exon) are significantly ($P < 0.01$) depleted of and gene bodies enriched with dDMPs. The lower panel shows the ratio of hypermethylated (gray bars) versus hypomethylated dDMPs (light bars) in different gene regions.

became transcriptionally downregulated during gestational development (Fig. 4). Since significant expression changes were seen in two different assays each, artifacts can be largely excluded.

The large (3428 of 6344) number of dDMPs with genome-wide significance in both studies but opposite direction of change does not necessarily reflect experimental artifacts. Different developmental time windows may account for a substantial fraction of these opposing dDMPs (o-dDMPs). Gestational age was significantly lower in the published data set (Spiers et al., 2015) than in our study (Table 2). When plotting methylation versus gestational age for o-dDMPs, 2971 show a U-shaped methylation dynamics, being downmethylated in the first and upmethylated in the second trimester (Fig. 2, lower panel). A smaller number of 457 o-dDMPs displayed a reverse U shape, being upmethylated in the first and downmethylated in the second trimester. This is consistent with the abundance of hypomethylated dDMPs in the published data set (Spiers et al., 2015) and of hypermethylated dDMPs in our study. The turning point for most o-dDMPs was around gestational week 15.

3.2. Chromosomal distribution and clustering of m-dDMPs

Fig. 5 shows the chromosomal distribution of hyper- and hypomethylated dDMPs. Compared to the number of analyzed CpGs on the array, chromosomes 1 and 10 are significantly (adjusted $P < 0.05$) enriched with hypermethylated and chromosome 22 with hypomethylated dDMPs. Chromosome 19 is significantly depleted of hypermethylated dDMPs. To test whether dDMPs are stochastically distributed or clustered in certain chromosome region, we first defined clusters containing 5 or more adjacent CpG sites on the array. Based on the array architecture, we identified 24,588 such CpG clusters,

covering a total of 231,788 CpGs (28.9% of all analyzed sites). To detect local enrichment of m-dDMPs mapping to these positional clusters, Fisher's exact test was calculated for each cluster separately. After multiple testing correction, 68 clusters showed a significant (adjusted $P < 0.05$) enrichment with m-dDMPs. Genomic coordinates of these clusters and the correlation between regional methylation and gestational age are presented in Supplementary Table S2. Most (88%) m-dDMP clusters are located in coding sequence, however when considering that most CpGs on the array interrogate gene regions, this is not a significant enrichment (Fisher's exact test). For visualization, the 280 m-dDMPs were plotted along the length of chromosomes (Fig. 6). It is noteworthy that all chromosomes apart from 9, 13, 18, and 21 are endowed with m-dDMP clusters.

3.3. Association of dDMPs with autism

Approximately half (1477 of 2913) of m-dDMPs are associated with genes. To test whether m-dDMPs are enriched in genes for neuropsychiatric disorders, we used published lists of 742 genes that have been associated with ASD (AutDB, 2015; Basu et al., 2009), 119 genes associated with schizophrenia (Schizophrenia Working Group of the Psychiatric Genomics Consortium, 2014), and 678 genes associated with Alzheimer's disease (AlzGene, 2015; Bertram et al., 2007). The only candidate gene set showing significant ($P < 0.0001$) enrichment with m-dDMP genes (96 of 742) was autism: 50 ASD candidate genes were associated with hypermethylated, 41 with hypomethylated, and 5 with both hypo- and hypermethylated m-dDMPs. A recent 450K methylation array study (Nardone et al., 2014) identified 5329 CpG sites with significant methylation changes in adult frontal cortex (BA10) of autistic patients, compared to controls. There is a highly significant ($N = 83$; $P < 0.0001$) overlap between CpGs that are differentially methylated in adult autistic frontal cortex (5329) and our m-dDMP marker set (2916). Even more interestingly, 7 of 8 hypomethylated m-dDMPs showed higher methylation and 70 of 75 hypermethylated m-dDMPs decreased methylation in the adult autistic brain. Another 450K array study (Ladd-Acosta et al., 2014) revealed three differentially methylated regions (with 74 CpG sites on the array) in adult temporal cortex of 19 autism cases versus 21 controls. One DMR with decreased methylation in the adult autistic brain was associated with *PPRT1*, which represents a hypermethylated m-dDMP gene in our study. This leads to a model that incomplete downmethylation and upmethylation, respectively, of m-dDMPs during fetal development persist into the adult brain and predisposes to autism (Fig. 7).

Recent work using 450K methylation arrays identified 2104 differentially methylated, mainly hypomethylated CpGs in adult frontal cortex from patients with schizophrenia (Jaffe et al., 2016). However, only one of these 2104 CpGs, cg16884940 in the *CCDC53* gene body, coincided with a m-dDMP in our study. Unlike autism, schizophrenia-associated CpGs (in adult brain) appear to be significantly ($P < 0.0001$) underrepresented in m-dDMPs.

3.4. M-dDMPs and human-specific changes in gene regulation during primate brain evolution

We defined a list (Supplementary Table S1) of 2357 protein-coding genes with human-specific brain expression patterns (Nowick et al., 2009; Liu et al., 2012; Florio et al., 2015) and 441 genes close to human-specific histone methylation signatures (Shulha et al., 2012). These genes which acquired human-specific regulation during brain evolution are significantly enriched with m-dDMP genes ($N = 255$; $P < 0.0001$). Because the functional relationship between DNA methylation and transcription is most well established for promoter regions, we concentrated further on genes with m-dDMPs in the promoters regions, exhibiting human-specific brain regulation. Eight of 2357 protein-coding genes, namely *AMOTL2*, *FAM19A5*, *IFIT2*, *IGFBP6*, *LARP1*, *MYO16*,

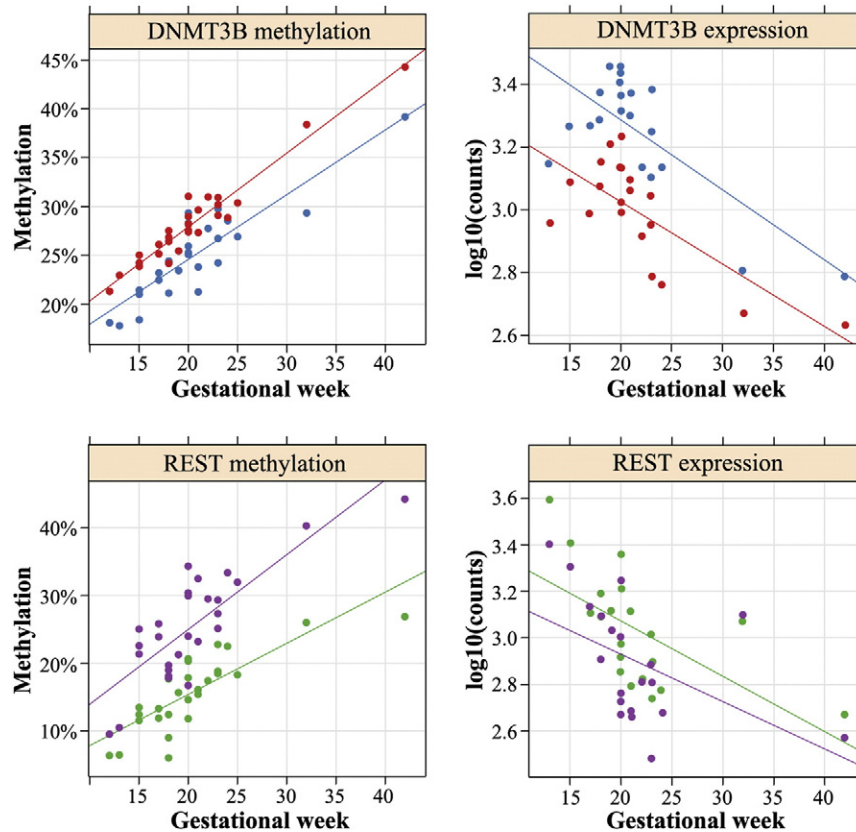


Fig. 4. Methylation and expression changes of *DNMT3B* (upper panel) and *NRSF/REST* (bottom panel) in the developing brain. Methylation was measured by Illumina 450K arrays and expression by targeted RNA sequencing. Each dot represents a fetal cortex sample. For methylation analysis, red and blue dots represent two m-dDMPs (cg22605822 and cg14224313) in *DNMT3B*, purple and green dots two m-dDMPs (cg25313468 and cg24291500) in *NRSF/REST*. Regression lines are calculated for each m-dDMP separately. For expression analysis, red and blue dots represent assays *DNMT3B_6699965* and *DNMT3B_6699954*, respectively, purple and green dots *REST_6968017* and *REST_6715088*, respectively.

OPCML, and *PHLDB1*, and 6 of 441 genes, *AMOTL2*, *GPRIN2*, *MUC5B*, *NFAM1*, *OPCML*, and *TMEM72*, with human-specific histone modifications are endowed with m-dDMP promoters. In addition, microRNAs which are differentially expressed in the human and primate brain (Hu et al., 2011) are significantly ($P < 0.0001$) enriched with m-dDMP promoters. Six of 153, *MIR219-2*, *MIR30A*, *MIR589*, *MIR1237*, *MIR193B*, and *MIRLET7C* are controlled by m-dDMP promoters. Altogether, 13 of 18 m-dDMP promoters become methylated, suggesting that the respective genes (*AMOTL2*, *FAM19A5*, *GRIN2*, *NFAM1*, *IGFBP6*, *LARP1*, *MYO16*, *PHLDB1*, and *TMEM72*) and miRNAs (*MIR30A*, *MIR193B*, *MIR219-2*, and *MIR1237*) are downregulated towards the end of pregnancy. Three genes (*IFIT2*, *MUC5B*, and *OPCML*) and two microRNAs (*MIR589* and *MIRLET7C*) become demethylated and likely activated during human fetal brain development.

4. Discussion

The mechanisms underlying human brain evolution and ontogeny are still far from being understood. In many respects, including size, speed of growth, gyrification and energy consumption, in particular during development, the human brain is outstanding (Vannucci and Vannucci, 2000; Ulijaszek, 2002; Sakai et al., 2012; Lewitus et al., 2013). Because the genetic differences between humans and chimpanzees are rather small (Varki and Altheide, 2005), it is plausible to assume that enhanced encephalization and cognitive abilities of the human brain are at least to some extent due to changes in gene regulation. The same epigenetic mechanisms which have been adapted for human brain evolution may also play a crucial role for ontogeny. Considering that epigenetic variation is much (at least one order of magnitude) higher than genetic variation (Bennett-Baker et al., 2003) and can be influenced by environmental factors (Feil and Fraga, 2012; El Hajj

et al., 2014), it may account for a large part of phenotypic variation. Accumulating evidence suggests that the methylome is highly dynamic during human brain development (Numata et al., 2012; Pidsley et al., 2014; Spiers et al., 2015; Jaffe et al., 2016). Disturbances in this orchestrated process can be expected to interfere with normal brain development and function.

One important goal of our study was to identify methylation markers, in particular in genes and promoter regions, that are continuously up- or downmethylated during fetal brain development. To this end, we compared our results to a conceptually related 450K methylation array study (Spiers et al., 2015) and only 2916 m-dDMPs with genome-wide significance and the same direction of change in both data sets were considered further. Because of legal and ethical restrictions (which differ between countries), there is only limited access to fetal brain samples and tissue quality is often not optimum. One limitation of our study is the relatively small sample size ($N = 27$). Most of our brain samples were from spontaneous or induced abortions due to amniotic infection or placental problems. Although we cannot exclude that the various pathologies and postmortem times (<24 h to 72 h) affect methylation patterns in individual samples, this does not explain the observed developmental trajectories. One advantage of our study is that all fetuses underwent autopsy by an experienced pediatric pathologist and frontal cortex tissue was dissected from a well-defined area (BA10), compared to published data on undissected brain tissue from different regions. In our experience, neuronal cells and non-neuronal cells cannot be reliably sorted from frozen fetal cortex using NeuN-specific antibodies, because they are not always immunostaining positive. One important difference between the two studies, which may account for the large number of o-dDMPs, is gestational age. The median age in our study was 20 gestational weeks (range 12–42), whereas in the published data set it was 13 weeks (range 3–26). The identified 1767 hypermethylated and 1149 hypomethylated m-

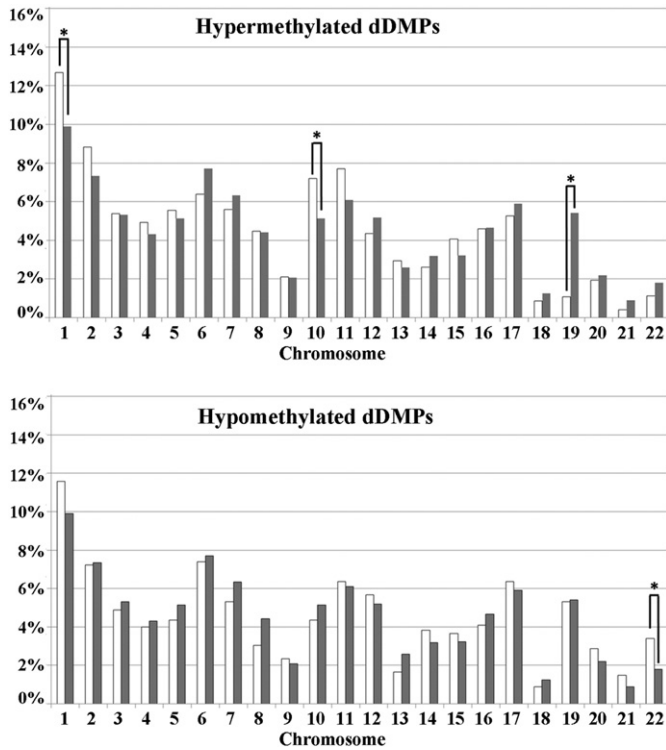


Fig. 5. Chromosomal distribution of hyper- and hypomethylated dDMPs, respectively. Gray bars represent the percentage of analyzed CpGs on a particular chromosome, white bars the percentage of hypermethylated (upper panel) versus hypomethylated (lower panel) dDMPs. Chromosomes 1 and 10 are significantly (adjusted $P < 0.05$) enriched with and chromosome 19 is depleted of hypermethylated dDMPs. Chromosome 22 is significantly enriched with hypomethylated dDMPs.

dDMPs matching between both studies are developmental trajectories continuously gaining and losing methylation, respectively, from early to late stages of pregnancy.

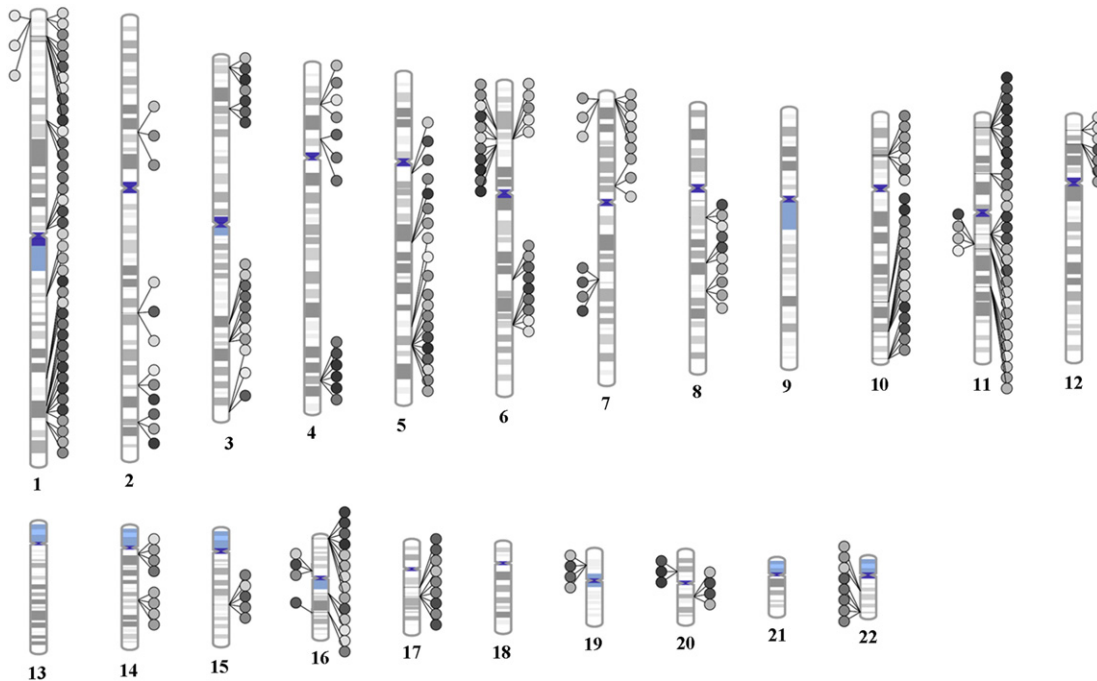


Fig. 6. 68 chromosomal regions are enriched with 280 m-dDMPs. Hypomethylated m-dDMPs are depicted as dots on the left side, hypermethylated m-dDMPs on the right side of the chromosomal ideograms. Shading indicates correlation between m-dDMP methylation and gestational age. Correlation coefficients range from -0.70 (light) to -0.91 (dark) and from 0.70 to 0.96 , respectively.

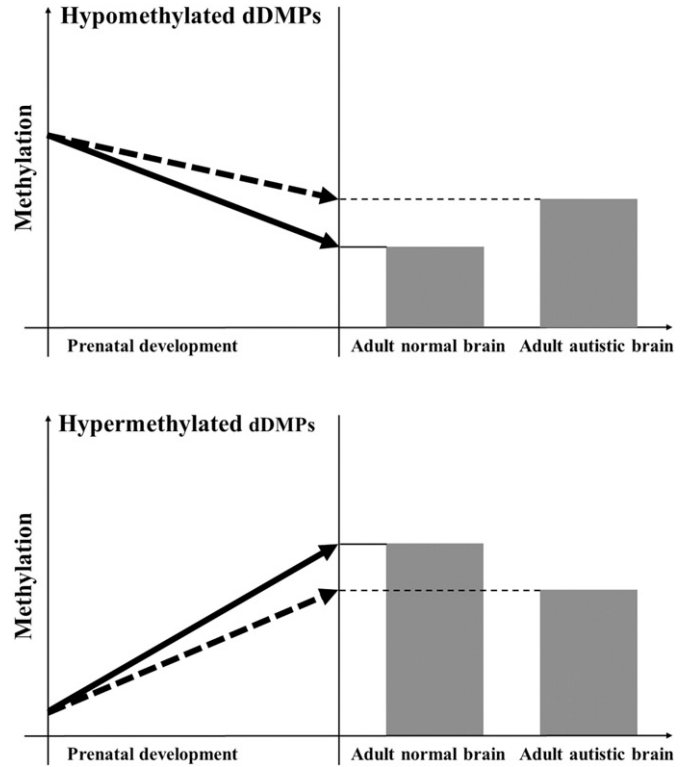


Fig. 7. Disturbances in methylation dynamics during fetal development, leading to increased methylation of hypomethylated m-dDMPs and decreased methylation of hypermethylated m-dDMPs in the autistic brain.

Several recent publications have linked dDMPs to neurodevelopmental disorders, in particular autism and schizophrenia (Pidsley et al., 2014; Spiers et al., 2015; Hannon et al., 2016). We have tested candidate gene sets for neurodevelopmental and neurodegenerative disorders for enrichment with m-dDMPs. Consistent with earlier

studies, m-dDMPs were enriched in genes that have been associated with autism. M-dDMPs in autism genes significantly overlapped with differentially methylated CpGs in the brain of adult autistic individuals (Ladd-Acosta et al., 2014; Nardone et al., 2014). Our observation that hypermethylated m-dDMPs are associated with hypomethylated regions in the adult autistic brain and vice versa suggests that reduced methylation dynamics during fetal brain development leads to persistent changes, which then may predispose to autism. Unlike autism, candidate genes for schizophrenia (Schizophrenia Working Group of the Psychiatric Genomics Consortium, 2014) and schizophrenia-associated CpGs (Jaffe et al., 2016) did not show significant enrichment with m-dDMPs.

Genes and microRNAs with dynamic promoter methylation during fetal brain development are prime candidates for human brain evolution. Among 105 m-dDMP promoters, we identified 12 genes and 6 microRNAs with human-specific regulation in the human compared to primate brains. Most of these promoters become methylated during human fetal brain development, consistent with transcriptional downregulation. The affected genes are involved in embryogenesis (*LARP1*), stem cell differentiation and proliferation (*NFAM1* and *TMEM72*), cell migration during development (*PHLDB1*), neurite growth (*GRIN2*), synaptic maturation (*AMOTL2*), and nervous system development (*MIR30A*, *IGFBP6*, *MYO16*).

One disadvantage of methylation array studies is that probes represent only 2% of all CpGs and are not equally distributed throughout the genome. Most probes are targeted across genes (promoter, 5' UTR, 1st exon, gene body, and 3' UTR) and CpG islands (including flanking CGI shores and shelves). However, even when correcting for the unequal coverage of interrogated CpGs across the linear genome, m-dDMPs appeared to cluster in particular chromosome regions. This supports the notion that developmental regulation (by DNA methylation) occurs not only at the individual gene level but also in larger chromosomal domains. The linear chromosomes are segmented into hundreds of topological domains and subdomains, ensuring coordinated gene expression (Bickmore and van Steensel, 2013). Some chromosomes (1, 10, and 22) were enriched with and others (19) depleted of m-dDMPs. Chromosomes 9, 13, 18, and 21 did not contain any m-dDMP clusters. In the case of 13, 18, and 21 this may be partially explained by their low gene content. Assuming that m-dDMP clusters play an important role in fetal brain development, the lack of such clusters may contribute to the viability of trisomies 13, 18, and 21 after birth.

5. Conclusions

Collectively, our results support the view that DNA methylation patterns are highly dynamic during human fetal brain (frontal cortex) development. During the first trimester the fetal brain is globally hypomethylated, whereas in the second and third trimester methylation increases. The identified 1767 hypermethylated and 1149 hypomethylated m-dDMPs are developmental trajectories continuously gaining and losing methylation, respectively, from early to late stages of pregnancy. We propose that these m-dDMPs have been adopted for both brain evolution and ontogeny.

Supplementary data to this article can be found online at <http://dx.doi.org/10.1016/j.gene.2016.07.058>.

Acknowledgment

This research did not receive any specific grant from funding agencies in the public, commercial, or non-for-profit sectors. The authors thank Dr. Fabian Müller at the MPI for Informatics, Saarbücken for help with the RnBeads pipeline.

References

Aryee, M.J., Jaffe, A.E., Corrada-Bravo, H., Ladd-Acosta, C., Feinberg, A.P., Hansen, K.D., Izarrry, R.A., 2014. *Minfi: a flexible and comprehensive Bioconductor package for*

the analysis of Infinium DNA methylation microarrays. *Bioinformatics* 30, 1363–1369.

Assenov, Y., Müller, F., Lutsik, P., Walter, J., Lengauer, T., Bock, C., 2014. Comprehensive analysis of DNA methylation data with RnBeads. *Nat. Methods* 11, 1138–1140.

Basu, S.N., Kollu, R., Banerjee-Basu, S., 2009. AutDB: a gene reference resource for autism research. *Nucleic Acids Res.* 37, D832–D836.

Bennett-Baker, P.E., Wilkowski, J., Burke, D.T., 2003. Age-associated activation of epigenetically repressed genes in the mouse. *Genetics* 165, 2055–2062.

Bertram, L., McQueen, M.B., Mullin, K., Blacker, D., Tanzi, R.E., 2007. Systematic meta-analyses of Alzheimer disease genetic association studies: the AlzGene database. *Nat. Genet.* 39, 17–23.

Bickmore, W.A., van Steensel, B., 2013. Genome architecture: domain organization of interphase chromosomes. *Cell* 152, 1270–1284.

Colantuoni, C., Lipska, B.K., Ye, T., Hyde, T.M., Tao, R., Leek, J.T., et al., 2011. Temporal dynamics and genetic control of transcription in the human prefrontal cortex. *Nature* 478, 519–523.

El Hajj, N., Schneider, E., Lehnen, H., Haaf, T., 2014. Epigenetics and life-long consequences of an adverse nutritional and diabetic intrauterine environment. *Reproduction* 148, R111–R120.

El Hajj, N., Dittrich, M., Böck, J., Kraus, T.F., Nanda, I., Müller, T., et al., 2016. Epigenetic dysregulation in the developing Down syndrome cortex. *Epigenetics* (Epub ahead of print, PMID 27245352).

Fatemi, S.H., Folsom, T.D., 2009. The neurodevelopmental hypothesis of schizophrenia, revisited. *Schizophr. Bull.* 35, 528–548.

Feil, R., Fraga, M.F., 2012. Epigenetics and the environment: emerging patterns and implications. *Nat. Rev. Genet.* 13, 97–109.

Florio, M., Albert, M., Taverna, E., Namba, T., Brandl, H., Lewitus, E., et al., 2015. Human-specific gene ARHGAP11B promotes basal progenitor amplification and neocortex expansion. *Science* 347, 1465–1467.

Haaf, T., 2006. Methylation dynamics in the early mammalian embryo: implications of genome reprogramming defects for development. *Curr. Top. Microbiol. Immunol.* 310, 13–22.

Hannon, E., Spiers, H., Viana, J., Pidsley, R., Burrage, J., Murphy, T.M., et al., 2016. Methylation QTLs in the developing brain and their enrichment in schizophrenia risk loci. *Nat. Neurosci.* 19, 48–54.

Hu, H.Y., Guo, S., Xi, J., Yan, Z., Fu, N., Zhang, X., et al., 2011. MicroRNA expression and regulation in human, chimpanzee, and macaque brains. *PLoS Genet.* 7, e1002327.

Jaenisch, R., Bird, A., 2003. Epigenetic regulation of gene expression: how the genome integrates intrinsic and environmental signals. *Nat. Genet.* 33, 245–254.

Jaffe, A.E., Shin, J., Collado-Torres, L., Leek, J.T., Tao, R., Li, C., et al., 2015. Developmental regulation of human cortex transcription and its clinical relevance at single base resolution. *Nat. Neurosci.* 18, 154–161.

Jaffe, A.E., Gao, Y., Deep-Soboslay, A., Tao, R., Hyde, T.M., Weinberger, D.R., Kleinman, J.E., 2016. Mapping DNA methylation across development, genotype and schizophrenia in the human frontal cortex. *Nat. Neurosci.* 19, 40–47.

Jones, P.A., 2012. Functions of DNA methylation: islands, start sites, gene bodies and beyond. *Nat. Rev. Genet.* 13, 484–492.

Ladd-Acosta, C., Hansen, K.D., Briem, E., Fallin, M.D., Kaufmann, W.E., Feinberg, A.P., 2014. Common DNA methylation alterations in multiple brain regions in autism. *Mol. Psychiatry* 19, 862–871.

Lambert, N., Lambot, M.A., Bilheu, A., Albert, V., Englert, Y., Libert, F., et al., 2011. Genes expressed in specific areas of the human fetal cerebral cortex display distinct patterns of evolution. *PLoS One* 6, e17753.

Laurent, L., Wong, E., Li, G., Huynh, T., Tsigos, A., Ong, C.T., et al., 2010. Dynamic changes in the human methylome during differentiation. *Genome Res.* 20, 320–331.

Law, C.W., Chen, Y., Shi, W., Smyth, G.K., 2014. Voom: precision weights unlock linear model analysis tools for RNA-seq read counts. *Genome Biol.* 15, R29.

Levine, M.E., Lu, A.T., Bennett, D.A., Horvath, S., 2015. Epigenetic age of the pre-frontal cortex is associated with neuritic plaques, amyloid load, and Alzheimer's disease related cognitive functioning. *Aging (Albany NY)* 7, 1198–1211.

Lewitus, E., Kelava, I., Huttner, W.B., 2013. Conical expansion of the outer subventricular zone and the role of neocortical folding in evolution and development. *Front. Hum. Neurosci.* 7, 424.

Liu, X., Somel, M., Tang, L., Yan, Z., Jiang, X., Guo, S., et al., 2012. Extension of cortical synaptic development distinguishes humans from chimpanzees and macaques. *Genome Res.* 22, 611–622.

Loke, Y.J., Hannan, A.J., Craig, J.M., 2015. The role of epigenetic change in autism spectrum disorders. *Front. Neurol.* 6, 107.

Lunnon, K., Mill, J., 2013. Epigenetic studies in Alzheimer's disease: current findings, caveats, and considerations for future studies. *Am. J. Med. Genet. B Neuropsychiatr. Genet.* 162B, 789–799.

Maksimovic, J., Gordon, L., Oshlack, A., 2012. SWAN: subset-quantile within array normalization for Illumina Infinium HumanMethylation450 BeadChips. *Genome Biol.* 13, R44.

Mendioroz, M., Do, C., Jiang, X., Liu, C., Darbary, H.K., Lang, C.F., et al., 2015. Trans effects of chromosome aneuploidies on DNA methylation patterns in human Down syndrome and mouse models. *Genome Biol.* 16, 263.

Miller, J.A., Ding, S.L., Sunkin, S.M., Smith, K.A., Ng, L., Szafer, A., et al., 2014. Transcriptional landscape of the prenatal human brain. *Nature* 508, 199–206.

Nardone, S., Sams, D.S., Reuveni, E., Getselter, D., Oron, O., Karpuj, M., Elliott, E., 2014. DNA methylation analysis of the autistic brain reveals multiple dysregulated biological pathways. *Transl. Psychiatry* 4, e433.

Nowick, K., Gernat, T., Almaas, E., Stubbs, L., 2009. Differences in human and chimpanzee gene expression patterns define an evolving network of transcription factors in brain. *Proc. Natl. Acad. Sci. U. S. A.* 106, 22358–22363.

Numata, S., Ye, T., Hyde, T.M., Guitart-Navarro, X., Tao, R., Wininger, M., Colantuoni, C., Weinberger, D.R., Kleinman, J.E., Lipska, B.K., 2012. DNA methylation signatures in

- development and aging of the human prefrontal cortex. *Am. J. Hum. Genet.* 90, 260–272.
- Pidsley, R., Viana, J., Hannon, E., Spiers, H.H., Troakes, C., Al-Saraj, S., et al., 2014. Methylomic profiling of human brain tissue supports a neurodevelopmental origin for schizophrenia. *Genome Biol.* 15, 483.
- Ritchie, M.E., Phipson, B., Wu, D., Hu, Y., Law, C.W., Shi, W., Smyth, G.K., 2015. Limma powers differential expression analyses for RNA-sequencing and microarray studies. *Nucleic Acids Res.* 43, e47.
- Sakai, T., Hirata, S., Fuwa, K., Sugama, K., Kusunoki, K., Makishima, H., Eguchi, T., Yamada, S., Ogihara, N., Takeshita, H., 2012. Fetal brain development in chimpanzees versus humans. *Curr. Biol.* 22, R791–R792.
- Schizophrenia Working Group of the Psychiatric Genomics Consortium, 2014n. Biological insights from 108 schizophrenia-associated genetic loci. *Nature* 511, 421–427.
- Shulha, H.P., Crisci, J.L., Reshetov, D., Tushir, J.S., Cheung, I., Bharadwaj, R., et al., 2012. Human-specific histone methylation signatures at transcription start sites in prefrontal neurons. *PLoS Biol.* 10, e1001427.
- Spiers, H., Hannon, E., Schalkwyk, L.C., Smith, R., Wong, C.C., O'Donovan, M.C., Bray, N.J., Mill, J., 2015. Methylomic trajectories across human fetal brain development. *Genome Res.* 25, 338–352.
- Ulijaszek, S.J., 2002. Comparative energetics of primate fetal growth. *Am. J. Hum. Biol.* 14, 603–608.
- Vannucci, R.C., Vannucci, S.J., 2000. Glucose metabolism in the developing brain. *Semin. Perinatol.* 24, 107–115.
- Varki, A., Altheide, T.K., 2005. Comparing the human and chimpanzee genomes: searching for needles in a haystack. *Genome Res.* 15, 1746–1758.
- Weber, M., Hellmann, I., Stadler, M.B., Ramos, L., Pääbo, S., Rebhan, M., Schübeler, D., 2007. Distribution, silencing potential and evolutionary impact of promoter DNA methylation in the human genome. *Nat. Genet.* 39, 457–466.
- Werling, D.M., Geschwind, D.H., 2013. Sex differences in autism spectrum disorders. *Curr. Opin. Neurol.* 26, 146–153.
- Yoder, J.A., Walsh, C.P., Bestor, T.H., 1997. Cytosine methylation and the ecology of intragenomic parasites. *Trends Genet.* 13, 335–340.
- Zafeiriou, D.I., Ververi, A., Dafoulis, V., Kalyva, E., Vargiami, E., 2013. Autism spectrum disorders: the quest for genetic syndromes. *Am. J. Med. Genet. B Neuropsychiatr. Genet.* 162B, 327–366.